Stem Cell Reports
Article

ISSCR

OPEN ACCESS

Efficient CRISPR/Cas9-Mediated Versatile, Predictable, and Donor-Free Gene Knockout in Human Pluripotent Stem Cells

Zhongliang Liu,[1,6] Yi Hui,[2,6] Lei Shi,[3,6] Zhenyu Chen,[1] Xiangjie Xu,[1] Liankai Chi,[1] Beibei Fan,[1] Yujiang Fang,[1] Yang Liu,[1] Lin Ma,[1] Yiran Wang,[1] Lei Xiao,[3] Quanbin Zhang,[1] Guohua Jin,[2,*] Ling Liu,[1,4,*] and Xiaoqing Zhang[1,4,5,*]

[1]Shanghai Tenth People's Hospital, and Neuroregeneration Key Laboratory of Shanghai Universities, Tongji University School of Medicine, Shanghai 200092, China
[2]Department of Anatomy and Neurobiology, the Jiangsu Key Laboratory of Neuroregeneration, Nantong University, 19 Qixiu Road, Nantong, Jiangsu 226001, China
[3]College of Animal Science and Zhejiang University School of Medicine, Zhejiang University, Hangzhou 310058, China
[4]Tongji University Advanced Institute of Translational Medicine, Tongji University School of Medicine, 1239 Siping Road, Shanghai 200092, China
[5]The Collaborative Innovation Center for Brain Science, Tongji University, Shanghai 200092, China
[6]Co-first author
*Correspondence: jguohua@ntu.edu.cn (G.J.), lliu@tongji.edu.cn (L.L.), xqzhang@tongji.edu.cn (X.Z.)
http://dx.doi.org/10.1016/j.stemcr.2016.07.021

SUMMARY

Loss-of-function studies in human pluripotent stem cells (hPSCs) require efficient methodologies for lesion of genes of interest. Here, we introduce a donor-free paired gRNA-guided CRISPR/Cas9 knockout strategy (paired-KO) for efficient and rapid gene ablation in hPSCs. Through paired-KO, we succeeded in targeting all genes of interest with high biallelic targeting efficiencies. More importantly, during paired-KO, the cleaved DNA was repaired mostly through direct end joining without insertions/deletions (precise ligation), and thus makes the lesion product predictable. The paired-KO remained highly efficient for one-step targeting of multiple genes and was also efficient for targeting of microRNA, while for long non-coding RNA over 8 kb, cleavage of a short fragment of the core promoter region was sufficient to eradicate downstream gene transcription. This work suggests that the paired-KO strategy is a simple and robust system for loss-of-function studies for both coding and non-coding genes in hPSCs.

INTRODUCTION

The use of human pluripotent stem cells (hPSCs) in studying human biology and disease requires precise genome-targeting methodologies. While different from mouse cells, gene targeting in either human embryonic stem cells (hESCs) or human induced pluripotent stem cells (hiPSCs) is found to be technically difficult (Capecchi, 2005; Hockemeyer and Jaenisch, 2010; Zwaka and Thomson, 2003). This situation is now much improved with the development of the custom-engineered nucleases (CENs) (Hendriks et al., 2016). CENs are designed to introduce site-specific double-strand breaks (DSBs) within the genome, which trigger DNA repair and therefore facilitate genetic engineering (Hendriks et al., 2016; Hsu et al., 2014). To date three CENs have been developed, among which the type II clustered regularly interspaced short palindromic repeats (CRISPR)/CRISPR-associated protein 9 (Cas9) system is increasingly preferred, based on its high efficiency and less laboriousness compared with zinc-finger nucleases and transcription activator-like effector nucleases (Ding et al., 2013b; Hou et al., 2013).

The type II CRISPR/Cas9 system relies on three components as follows: the DNA nuclease Cas9, the CRISPR RNA (crRNA), and *trans*-activating crRNA (tracrRNA) (Jinek et al., 2012). To facilitate laboratory use, a single guide RNA (gRNA), which is encoded by a single vector plasmid (Cho et al., 2013; Cong et al., 2013; Mali et al., 2013), has now replaced the crRNA/tracrRNA duplex. The gRNA contains a 15- to 23-bp target DNA-matching sequence immediately upstream of a protospacer adjacent motif (PAM) (Fu et al., 2014; Hsu et al., 2013; Stemmer et al., 2015). The CRISPR/Cas9 derived from *Streptococcus pyogenes* is the most widely used system and has a 5′-NGG-3′ PAM (Cong et al., 2013; Mali et al., 2013). The 15- to 23-bp-long complementary sequence binds to the target genomic locus through strict Watson-Crick pairing (Fu et al., 2014; Hsu et al., 2013; Stemmer et al., 2015), where the gRNA directs Cas9 for DNA cleavage and therefore results in a DSB at a desired site (Jinek et al., 2012). A DSB introduced into the genome will initiate DNA repair through either error-prone non-homologous end joining (NHEJ) or homology-directed repair (HDR) in the presence of exogenous DNA templates (Geisinger et al., 2016; Heyer et al., 2010; Jasin and Rothstein, 2013; Lackner et al., 2015).

Both NHEJ and HDR have been used in hPSCs for gene editing (Byrne et al., 2015; Chen et al., 2014b; Ding et al., 2013a; Ding et al., 2013b; Genga et al., 2015; Hockemeyer et al., 2011; Hou et al., 2013; Kleinstiver et al., 2016; Slaymaker et al., 2016). For targeted gene knockout in hPSCs, NHEJ usually causes unpredicted insertions/deletions (indels), which makes the validation process technically troublesome and always generates unpredictable non-naturally existent proteins because of the frameshift

introduced (Chen et al., 2015; Gonzalez et al., 2014). In addition, NHEJ cannot be applied for efficient knockout of non-coding RNAs. For HDR-mediated gene knockout in hPSCs, a recombination donor, which consists of the 5′ homology arm, an exon-replacing module and/or drug-resistant selection module, and the 3′ homology arm, is required for proper homologous recombination. Although outcome is predictable, the targeting efficiency of the HDR-based system is low and variable (Giudice and Trounson, 2008; Hockemeyer and Jaenisch, 2010; Mali and Cheng, 2012; Zwaka and Thomson, 2003). Moreover, the requirement for construction of the multimodule donor vector renders this system time consuming and labor intensive.

Here, we report an efficient paired gRNA-guided CRISPR/Cas9 knockout (paired-KO) method in hPSCs. Introducing a pair of gRNAs and Cas9 into hPSCs caused two DSBs, which were subsequently repaired with precise ligation without indels. Since each gRNA/Cas9 cleaves the targeting sequences between positions −3 and −4 upstream of the PAM sequence in a predictable manner, this paired gRNA strategy can serve as a powerful tool for coding gene knockout as long as the DSBs are designed shortly downstream of the ATG start codon and the frameshift triggers an immediate premature translation termination codon (PTC) downward. The paired-KO method also worked well for multiplexable gene targeting, and was equivalently efficient for lesion of microRNA (miRNA) and long non-coding RNA (lncRNA). We therefore conclude that the current paired-KO strategy is a rapid, robust, outcome-predictable, and multiplexable genome-editing methodology, which benefits loss-of-function studies of both coding and non-coding genes in hPSCs.

RESULTS

Paired-KO Represents a Robust and Predictable Strategy for Gene Knockout in hPSCs

CRISPR/Cas9-introduced DSB mostly initiates NHEJ for DNA repair in the absence of recombination donors and is thus applied for gene lesion or mutation in cultured cells and animal models (Chen et al., 2015; Cong et al., 2013; Gonzalez et al., 2014; Shalem et al., 2014; Wang et al., 2014). It has been reported that introducing two DSBs could potentially increase the gene-targeting efficiency or induce genomic DNA-fragment deletion (Canver et al., 2014; Kang et al., 2015; Mandal et al., 2014; Zhang et al., 2015; Zheng et al., 2014). To ablate *SMAD3* in hESCs, we designed two adjacent gRNAs in exon 3 of *SMAD3* genome immediately downstream of the ATG start codon (Figure 1A). Both gRNAs and CAG promoter-driven Cas9-P2A-GFP vector were then co-electroporated into H9 hESCs together with a transient puromycin expression vector. Puromycin was added to the cells from day 2 to day 5 for a short period of selection, and drug-resistant clones were picked up and amplified for genomic DNA PCR analyses (Figure 1B). The predicted cleavage site of each complementary target region is between positions −3 and −4 relative to the PAM sequence, and for the two gRNAs designed for *SMAD3* the interspace between these two cleavage sites is 44 bp long. We obtained 11 puromycin-resistant colonies, and genomic PCR analyses using primer sets flanking the two cleavage sites verified that seven colonies (7/11, 63.6%) showed biallelic genomic DNA deletion, while four (4/11, 36.4%) remained intact (Figure 1B). Western blotting confirmed that all seven colonies with genomic DNA deletion lacked SMAD3 expression, while all four uncut colonies expressed similar levels of endogenous SMAD3 (Figure 1B). We then performed Sanger sequencing for all seven cut PCR fragments, the results of which showed that in six colonies the cleavage sites were exactly between −3 and −4 bases upstream of both PAMs and that the cleaved blunt-ended genome DNAs were precisely ligated without indels (Figures 1C and S1A). One exception was colony #8, which showed one allele with indels after NHEJ (Figure S1A).

We spent 3 days on *SMAD3* gRNAs cloning, 10 days on colony formation after electroporation, and 5 days on cell expansion before genotyping analysis. Therefore, we obtained *SMAD3* KO hESC lines within 20 days, which was much less laborious than our previous gene knockout strategy based on HDR (Chi et al., 2016). Moreover, two additional aspects make this paired-KO strategy even more fascinating. First, the biallelic gene-targeting efficiency was extremely high and there was no monoallelic gene deletion verified in this case. Second, different from results obtained from other mammalian cells, which frequently incorporated indels during the DNA repair process (Gonzalez et al., 2014), paired-KO hESCs showed predicted target-site cleavage and precise end joining without indels. We also designed another primer pair to extend the genomic DNA PCR fragment, whose results showed that the amplified 1,385-bp DNA products equally remained in all clones, suggesting that no large DNA fragments were deleted (Figures S1B and S1C). Therefore, paired-KO is more predictable and controllable than conventional strategies induced by single DSB-triggered NHEJ. Via careful gRNA selection in controlling the site and length of the DNA fragments designed for deletion, PTCs can be easily introduced, and the engineered mRNAs with PTCs targeted for degradation through the nonsense-mediated decay (NMD) pathway (Brogna and Wen, 2009; Fatscher et al., 2015; Lykke-Anderson and Jensen, 2015). Indeed, qPCR analysis showed 50% downregulation of *SMAD3* mRNA in knockout cells compared with the wild-type counterpart (Figure 1D). Therefore, the current paired-KO strategy is

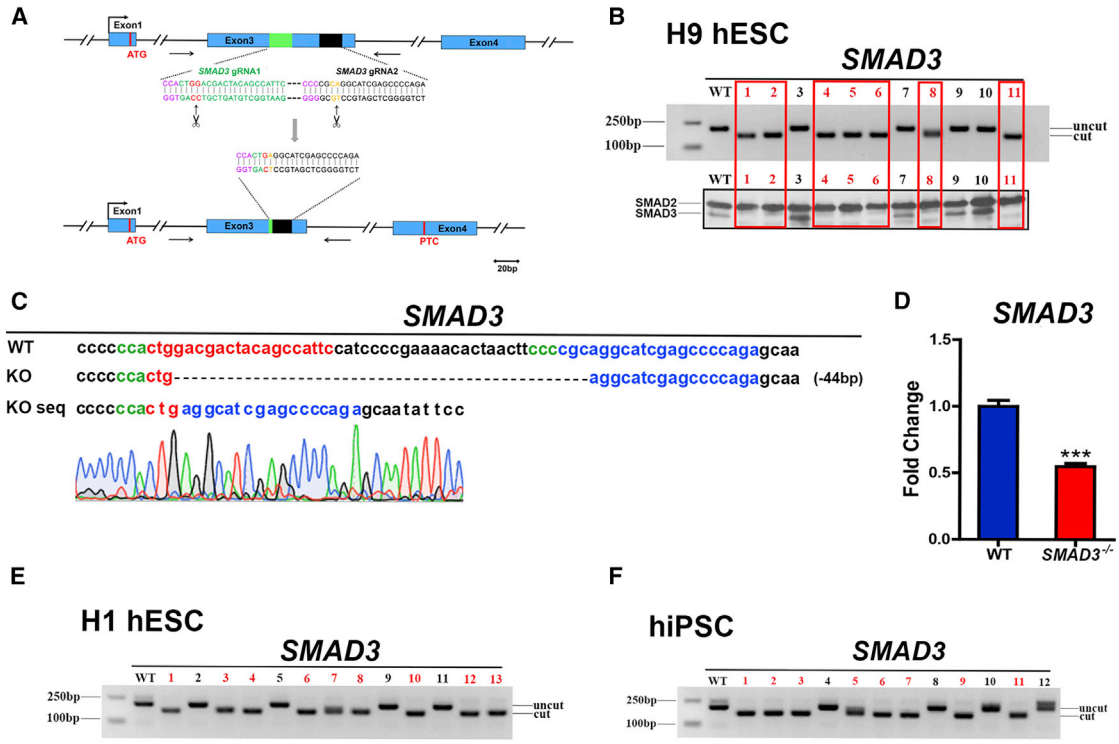

Figure 1. Efficient *SMAD3* Knockout in hPSCs through Paired-KO

(A) Schematic representation of the paired-KO strategy for *SMAD3* knockout. The cleavage sites are pointed out by the scissors and arrows. The PAM sequences are in purple. The positions of the designed primers for genomic PCR are shown as arrows. PTC, premature translation termination codon.

(B) Eleven colonies retrieved from *SMAD3* paired-KO in H9 hESCs. The top panel shows the genomic DNA PCR results and the lower panel shows western blotting results immunoblotted with the anti-SMAD2/3 antibody. Biallelically targeted colonies are labeled in red.

(C) Genomic DNA sequences before and after the paired gRNA-mediated cleavage and repair. A representative Sanger sequencing peak map verifies precise rejoining of the double blunt ends.

(D) qPCR data show decreased *SMAD3* mRNA expression in the biallelically targeted colonies. Data are presented as mean ± SEM of three independent experiments. ***$p < 0.001$, unpaired two-tailed Student's t test.

(E and F) Efficient *SMAD3* targeting in H1 hESCs (E) and hiPSCs (F) through paired-KO. Biallelically targeted colonies are labeled in red. See also Figure S1.

more predictable and does not culminate in non-natural proteins, which may exhibit unexplainable biological functions.

To test whether the paired-KO strategy could be applied to other PSC lines, we performed the same experiment in H1 hESCs and hiPSCs (Hu et al., 2010). Again, the biallelic targeting efficiencies were 69.23% (9/13) and 66.67% (8/12) in H1 hESCs and hiPSCs, respectively (Figures 1E and 1F). Sanger sequencing data also confirmed that blunt ends were ligated without indels in both cell lines (Figure S1D).

Off-target effects are major concerns for applying CENs in genetic engineering. Introducing two gRNAs in the cells could possibly increase the off-target effects. We therefore analyzed the integrity of the potential off-target sites predicted by the online program designed by Zhang's laboratory (http://crispr.mit.edu/) through Sanger sequencing. As shown in Figures S1E and S1F, five principal suspected off-target sites for each gRNA remained intact in a randomly picked biallelically targeted colony. These data suggest that the off-target effect is not a major issue for paired-KO.

We next repeated this paired-KO paradigm by targeting *CTNNB1* in hPSCs (Figure 2A). After electroporation and puromycin selection, 16 colonies were retrieved. Genomic DNA PCR results confirmed that six colonies were biallelically targeted, compared with only one monoallelic targeting colony and one mistargeted colony (Figure 2B). Western blotting and immunostaining experiments showed complete lack of CTNNB1 protein expression in the biallelically targeted lines (Figures 2C and 2D). Sanger sequencing and large DNA-fragment

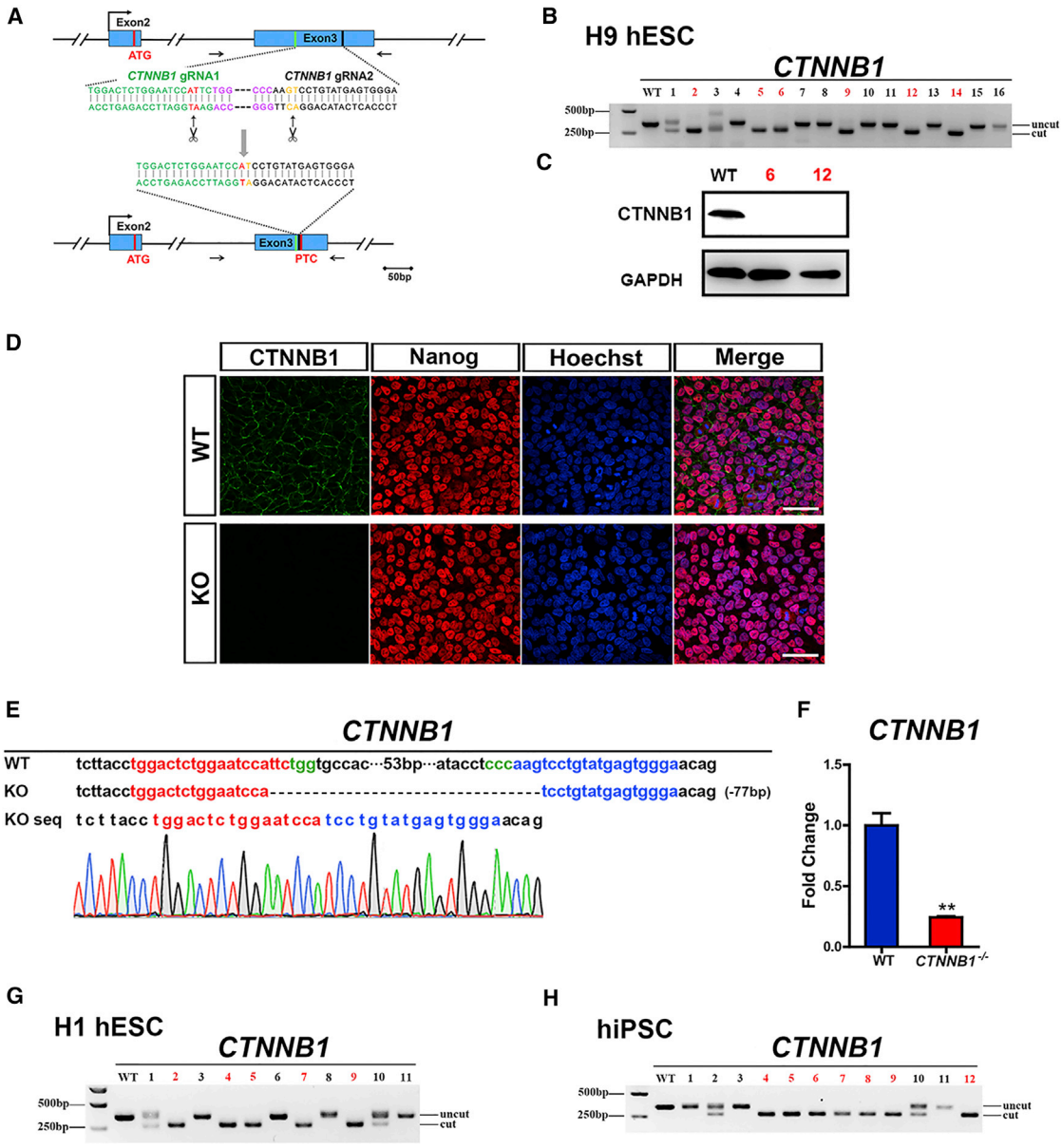

Figure 2. Efficient *CTNNB1* Knockout in hPSCs through Paired-KO

(A) Schematic representation of the paired-KO strategy for *CTNNB1* knockout.

(B) Genomic DNA PCR results of 16 colonies retrieved from *CTNNB1* paired-KO in H9 hESCs. Biallelically targeted colonies are labeled in red.

(C) Western blotting experiments confirm complete lack of CTNNB1 protein expression in biallelically targeted colonies.

(D) Confocal images show CTNNB1 and Nanog expression in wild-type (WT) and *CTNNB1* knockout (KO) H9 hESCs by immunostaining. Scale bar, 50 μm.

(E) Genomic DNA sequences before and after the paired gRNA-mediated cleavage and repair. A representative Sanger sequencing peak map verifies precise rejoining of the double blunt ends.

(F) qPCR data show decreased *CTNNB1* mRNA expression in the biallelically targeted colonies. Data are presented as mean ± SEM of three independent experiments. **$p < 0.01$, unpaired two-tailed Student's t test.

(G and H) Efficient *CTNNB1* targeting in H1 hESCs (G) and hiPSCs (H) through paired-KO. Biallelically targeted colonies are labeled in red. See also Figure S2.

Table 1. Targeting Efficiencies of 14 Protein-Encoding Genes of Interest through Paired-KO in H9 hESCs

Gene	Clone Number	Targeted Number	Biallelically Targeted Number	Targeting Efficiency (%)	Biallelically Targeted Efficiency (%)
ADM	19	12	8	63.16	42.11
BHLHE40	17	11	7	64.71	41.18
DDIT4	26	24	13	92.31	50.00
GLUT3	16	8	3	50.00	18.75
SHISA3	19	17	10	89.47	52.63
CTNNB1	16	7	6	43.50	37.50
SMAD3	31	19	13	61.29	41.94
MAF	18	9	8	50.00	44.44
SP8	15	5	5	33.33	33.33
MEIS2	5	2	2	40.00	40.00
TP53	23	20	18	86.96	78.26
NF1	23	18	13	78.26	56.52
ASCL1	43	41	31	95.35	72.09
FOXG1	8	6	6	75.00	75.00

See also Figures S3 and S4.

PCR amplification further revealed precise ligation of the double-cleaved blunt ends (Figures 2E and S2A–2D). Moreover, *CTNNB1* mRNA level in biallelically targeted lines decreased up to 75%, further indicating an NMD response (Figure 2F). In addition, biallelic targeting of *CTNNB1* in H1 hESCs and hiPSCs was also achieved with high efficiency (Figures 2G and 2H). Again, we did not find any off-target mutations in the predicted off-target sites (Figures S2E and S2F).

We also designed another ten pairs of gRNAs targeting cell-cycle regulators, glucose transporters, or transcription factors related to lineage development (Table 1 and Figure S3). With just one single attempt, we successfully obtained all desired knockout hESC lines. Among the total colonies counted, the percentage of lines showing at least one-allele gene targeting ranged from 33.33% to 95.35%, while the biallelic targeting efficiency ranged from 18.75% to 75.00% (Table 1). For each gene knockout, we sequenced two to three genomic DNA PCR-amplified fragments, and found that they were all precisely repaired (Figure S3). We screened all genes targeted for potential SNPs and found that *MAF*, *GLUT3*, and *SHISA3* had both SNPs within a range of 5 kb upstream or 5 kb downstream of the cleavage sites in H9 hESCs. We then sequenced all *MAF*, *GLUT3*, and *SHISA3* knockout colonies, the results of which showed that all colonies retained both upstream and downstream SNPs, indicating that no large genome fragments were deleted during the paired gRNA-mediated gene targeting.

One-Step Targeting of Multiple Genes with the Paired-KO Strategy

Given its high efficiency for biallelic gene targeting, we investigated whether the paired-KO strategy could be used for targeting of multiple genes simultaneously. *NF1* and *TP53* are two tumor-suppressor genes whose loss of function is closely related to many malignant tumors. We designed paired gRNAs targeting exon2 of *NF1* and exon1 of *TP53*, respectively, which were all closely downstream of the ATG start codon (Figure 3A). All four gRNAs were electroporated into H9 hESCs with Cas9. After puromycin selection, we retrieved a total of 22 colonies. Genomic PCR results showed that for *NF1*, 13 out of 22 colonies showed biallelic DNA deletion, while 18 of 22 colonies had biallelic deletions for *TP53* (Figure 3B). Among the 13 correctly targeted colonies for *NF1*, 11 were also biallelically targeted at the *TP53* loci, demonstrating a 50% double-knockout efficiency (Figures 3B and 3F). TP53, but not NF1, is expressed in hESCs and, indeed, the biallelically targeted #4, #16, and #19 colonies showed no endogenous TP53 expression (Figure 3C). Sequencing results confirmed that the cleavage sites were just as expected, and the end-joining sites did not have any indels (Figure 3D). We then differentiated wild-type or double-knockout lines toward

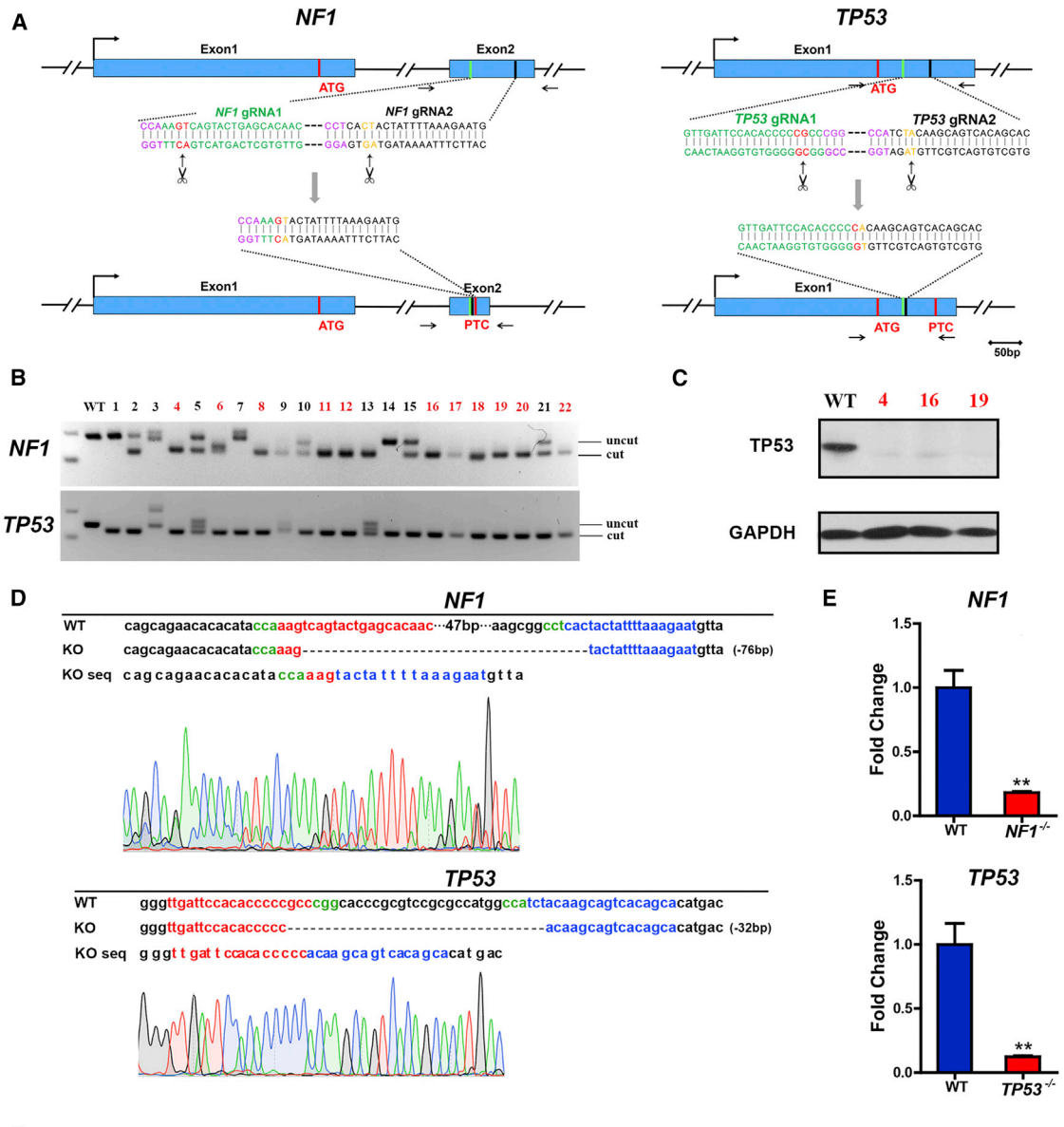

F

Gene	Number of clones	*NF1* targeted	*TP53* targeted	*NF1/TP53* targeted	Biallelically *NF1/TP53* targeted	*NF1/TP53* targeting efficiency(%)	Biallelic *NF1/TP53* targeting efficiency(%)
NF1 *TP53*	22	20	22	20	11	90.91%	50.00%

Figure 3. One-Step *NF1* and *TP53* Knockout in hESCs through Paired-KO

(A) Schematic representation of the paired-KO strategy for double knockout of *NF1* and *TP53* through one-step manipulation in hESCs.

(B) Genomic DNA PCR results of 22 colonies retrieved from H9 hESCs subjected to one-step targeting for both *NF1* and *TP53*. Lines with both *NF1* and *TP53* biallelically targeted are labeled in red.

(C) Western blot shows complete TP53 knockout in the biallelically targeted lines.

(legend continued on next page)

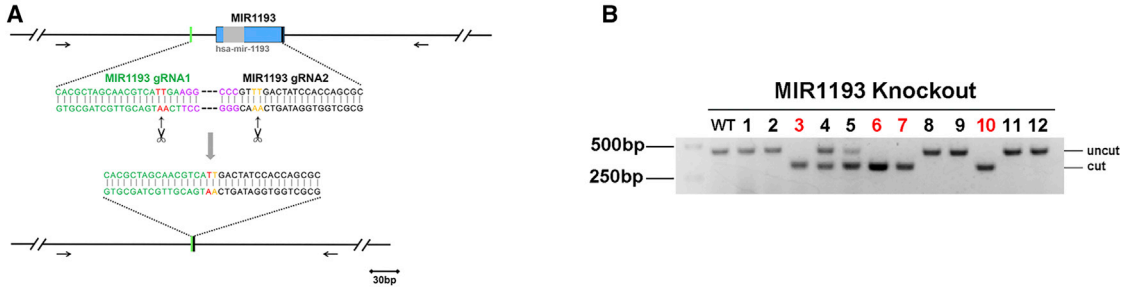

Figure 4. Targeting miRNA in hESCs through Paired-KO

(A) Schematic representation of the paired-KO strategy for MIR1193 knockout in hESCs.

(B) Genomic DNA PCR results show the monoallelic or biallelic deletion of MIR1193 in hESCs. Biallelically targeted colonies are labeled in red.

a neural fate for 25 days with a well-established protocol (Chi et al., 2016; Zhang et al., 2010), and qPCR analyses revealed a significant decay of both *NF1* and *TP53* mRNAs (Figure 3E).

Non-coding RNA Knockout via Paired-KO

Non-coding RNAs, including miRNAs and lncRNAs, play important roles in hPSC maintenance and lineage differentiation (Ivey and Srivastava, 2010; Jia et al., 2013; Pauli et al., 2011). Since the open-reading-frame frameshift mediated by the traditional NHEJ strategy is not sufficient to ablate the expression of a non-coding RNA, antisense and RNAi are widely used methods for downregulating their expression, although with still controversial efficacy. For gene targeting we first chose MIR1193, located at chromosome 14, whose biological functions remain to be investigated. Two gRNAs flanking MIR1193 loci were designed and then electroporated into H9 hESCs with Cas9 (Figure 4A). Drug-resistant colonies were then validated by genomic PCR. Our results showed that 4 out of 12 colonies showed biallelic deletions, suggesting that miRNAs can be knocked out in hESCs through the paired-KO strategy as efficiently as protein-encoding genes (Figure 4B).

lncRNAs are defined as transcripts longer than 200 nucleotides without protein-coding potentials. The fragments we deleted for gene knockout described above via the paired-KO strategy were within 500 bp, so it remained unclear whether there is any tolerance for genomic DNA deletion related to the distance in between the double DSBs in hPSCs. *MALAT1* is an lncRNA proposed to play a role in tumor metastasis, which is coded by just one exon longer than 8,000 bp (Gutschner et al., 2013). We designed five gRNAs whose target sites relative to the transcriptional start site (TSS) were about 0 bp (gRNA1), +500 bp (gRNA2), +1,000 bp (gRNA3), +3,000 bp (gRNA4), and +8,000 bp (gRNA5), respectively (Figure 5A). We then paired gRNA1 with each of the others and electroporated them in H9 hESCs to delete fragments of different length. gRNA1/2, gRNA1/3, and gRNA1/4 successfully yielded biallelic deletions with high efficiency, suggesting that the paired-KO strategy could be used to delete up to 3,000 bp of DNA fragments in the genome of hPSCs (Figures 5B–5D). However, in the gRNA1/5 pair designed to delete the entire lncRNA, only monoallelic targeting colonies were identified and no homozygous knockout colonies were successfully generated (Figure 5E).

Sanger sequencing further validated that in all four gRNA pairs, the double blunt ends were largely ligated with no indels, regardless of the length of deleted DNA fragments (Figure 5F). However, these results indicate an inverse relationship between the deletion size and deletion efficiency (Figure 5G). To fully eliminate *MALAT1* expression, we constructed another gRNA (gRNA0), which targeted a locus 1,000 bp upstream of the TSS; this 1,000-bp-long DNA fragment belongs to the core promoter region of *MALAT1* (Figure 5A). The gRNA0/1 pair was then electroporated into hESCs, and genomic PCR showed that among the six colonies chosen, three were biallelically targeted and one was monoallelically targeted (Figure 5H). qPCR analyses were then used to verify the mRNA expression levels of *MALAT1* among all these six colonies. The colonies with biallelic 1,000-bp promoter deletion almost completely lacked mRNA expression, while the monoallelically

(D) Genomic DNA sequences before and after the paired gRNA-mediated cleavage and repair in *NF1* and *TP53* loci. Sanger sequencing data of a double-knockout line confirm the precise ligations of the double blunt ends for both *NF1* and *TP53*.

(E) qPCR data show decreased NF1 and TP53 mRNA expression in day-25 neural differentiation derivatives from the double-knockout lines. Data are presented as mean ± SEM of three independent experiments. $^{**}p < 0.01$, unpaired two-tailed Student's t test.

(F) Genome-targeting efficiency of *NF1* and *TP53*.

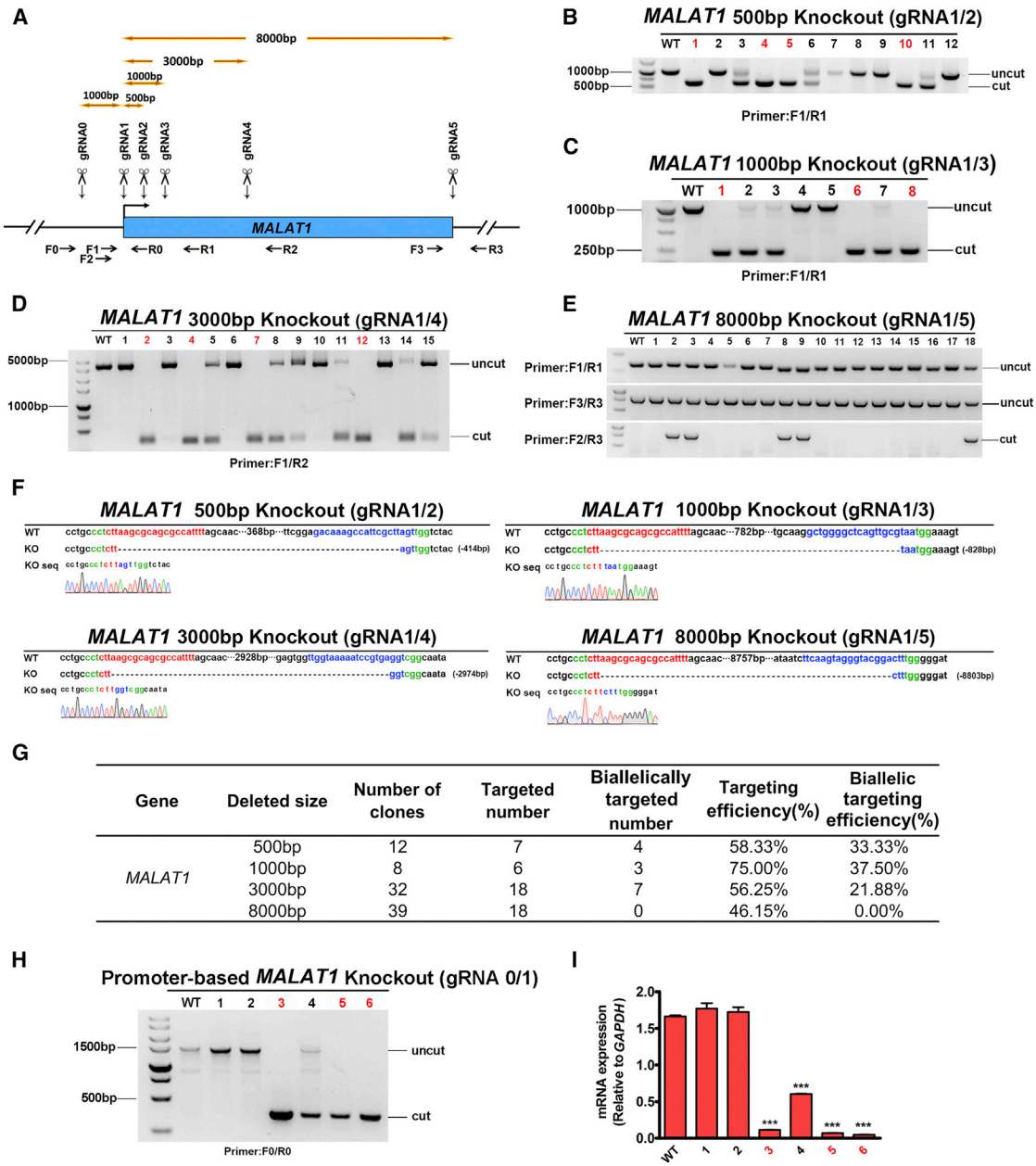

Gene	Deleted size	Number of clones	Targeted number	Biallelically targeted number	Targeting efficiency(%)	Biallelic targeting efficiency(%)
MALAT1	500bp	12	7	4	58.33%	33.33%
	1000bp	8	6	3	75.00%	37.50%
	3000bp	32	18	7	56.25%	21.88%
	8000bp	39	18	0	46.15%	0.00%

Figure 5. Targeting lncRNA in hESCs through Paired-KO

(A) Schematic representation of the paired-KO strategy for *MALAT1* knockout in hESCs. Six gRNAs targeting different loci are designed and gRNA1 is paired with the remaining five gRNAs for deletion of desired fragments with different sizes. Forward and reverse primers are indicated by arrows.

(B) Genomic DNA PCR results show the monoallelic or biallelic deletion of the proximal 500-bp exon fragment of *MALAT1* through gRNA1/2 combination. Biallelically targeted colonies are labeled in red.

(C) Genomic DNA PCR results show the monoallelic or biallelic deletion of the proximal 1,000-bp exon fragment of *MALAT1* through gRNA1/3 combination. Biallelically targeted colonies are labeled in red.

(D) Genomic DNA PCR results show the monoallelic or biallelic deletion of the proximal 3,000-bp exon fragment of *MALAT1* through gRNA1/4 combination. Biallelically targeted colonies are labeled in red.

(E) Genomic DNA PCR results show the paired gRNA/Cas9 yield monoallelic deletion of the entire ~8,000-bp exon fragment of *MALAT1* through gRNA1/5 combination.

(F) Sanger sequencing data show precise ligation in all four types of gRNA pairs with different deletion sizes.

(legend continued on next page)

targeted colony remained at half of the lncRNA gene expression (Figure 5I). These data suggest that promoter-based gene targeting may serve as an alternative method for efficient lesion of genes, especially large lncRNAs.

DISCUSSION

Double gRNAs have been used to increase the gene-targeting efficiencies in either gene ablation or exogenous donor-based HDR (Chen et al., 2015; Hsu et al., 2014; Kang et al., 2015; Mandal et al., 2014; Zheng et al., 2014). It has also been reported that two adjacent DSBs could be used to create a deletion of the intervening fragment in both cultured cell lines and model organisms (Canver et al., 2014; Lee et al., 2010; Song et al., 2016; Zhang et al., 2015). In some reports, the two DSBs were repaired through NHEJ and indels were sometimes introduced (Canver et al., 2014; Chen et al., 2014a, 2014c; Ho et al., 2015; Lv et al., 2016; Zhou et al., 2014). In our current study, the paired-KO triggered DSBs are mostly ligated through direct end joining without indels in hPSCs. When Byrne et al. (2015) pioneered an experiment for replacing human *THY1* gene with its mouse homolog through double gRNAs/Cas9-mediated cleavage in hiPSCs, they also found DNA-fragment deletion in between the two cleaved sites and rejoining of the blunt ends without indels. This precise NHEJ or precise gene deletion after paired gRNA-mediated DSBs has also been observed in HEK293 cells and hematopoietic stem cells (Geisinger et al., 2016; Ho et al., 2015; Mandal et al., 2014; Zheng et al., 2014). Given these predictable virtues of DNA cleavage and repair paradigms mediated by double gRNAs, the current paired-KO strategy is suitable for gene knockout in hPSCs without generating any non-natural proteins. Moreover, this paired gRNA strategy could also be used to delete a specific genomic fragment in hPSCs with designated *cis*-regulatory DNA element deletion, protein domain deletion, protein truncation, or mutation.

Another application of the paired-KO strategy is to ablate lncRNA expression in hPSCs. While >100-kb fragments have been successfully deleted in cell lines and animals (Canver et al., 2014; Chen et al., 2014c; Xiao et al., 2013; Zhang et al., 2015), we find that DNA fragments larger than 8 kb exhibit extremely low efficiency for gene targeting in hPSCs. Therefore, we offered two alternative ways for ablating the expression of lncRNA. For deletion of a short lncRNA or a small fragment within a large piece, direct DNA deletion through paired-KO works as efficiently as with coding genes, while for a large lncRNA itself, removal of the core promoter region may be more practical for complete loss-of-function analysis.

In summary, we report that the paired-KO strategy is an efficient, outcome-predictable, and multiplexable genome-editing methodology, suitable for loss-of-function studies of both coding and non-coding genes in hESCs and hiPSCs.

EXPERIMENTAL PROCEDURES

hPSC Culture

hESCs (H9, WA09 or H1, WA01, passages 25–45, WiCell Agreement No. 14-W0377) were maintained on mouse embryonic fibroblast (MEF) feeder in a hESC culture medium as we previously described (Chi et al., 2016; Zhang et al., 2010). The components of the hESC culture medium (hESCM) are: DMEM/F12, 20% Knockout serum replacer, 1× minimal essential medium (MEM) non-essential amino acids solution, 1× L-glutamine solution, 0.1 mM β-mercaptoethanol, and 4 ng/mL fibroblast growth factor 2. Cells were passaged every 5 days through dispase (Gibco, 17105) digestion and the medium was changed every day. The hiPSCs line used in this study has been reported in our previous paper (Hu et al., 2010).

Neural Differentiation of hPSCs

The detailed procedure for neural differentiation of hPSCs was described previously (Zhang et al., 2001, 2010). In brief, after dispase digestion, hPSCs were removed from the MEF layers and then pipetted up and down against the bottom of a 50-mL conical centrifuge tube to break up the hPSC clusters into 100- to 200-μM pieces. Within the first 4 days, hESCs were suspended in hESCM to form embryoid bodies and medium was then switched to the neural induction medium to induce the cells toward a neuroectoderm fate. At day 6 post differentiation, cell aggregates were plated down on a laminin-coated culture surface. At day 17, neural progenitor cells were detached from the plate and maintained in suspension to form neurospheres. The recipe for NIM is as follows: DMEM/F12, 1× N2 supplement, 1× MEM non-essential amino acids solution, and 2 μg/mL heparin.

Construction of the gRNA Plasmids

The blank gRNA vector with two BbsI restriction sites was as described previously (Chen et al., 2015). The gRNA vector was digested with BbsI, gel purified, and ligated to the annealed oligos containing targeting sequences of designed gRNAs. For the

(G) An inverse relationship between targeting efficiency and deletion size.
(H) Genomic DNA PCR results show the monoallelic or biallelic deletion of the 1,000-bp promoter region of *MALAT1* through gRNA0/1 combination. Biallelically targeted colonies are labeled in red.
(I) qPCR results show the mRNA expression levels of *MALAT1* in wild-type, heterozygous, or homozygous knockout colonies. Data are presented as mean ± SEM of three independent experiments. ***$p < 0.001$, unpaired two-tailed Student's t test.

detailed gRNA sequences for each gene, see Supplemental Experimental Procedures.

Generation of Knockout hPSC Lines

hPSCs were cultured in hESCM with 1 mM Y-27632 (Calbiochem, Y27632), a Rho kinase inhibitor, for 3 hr prior to electroporation. Cells were then digested by trypsin for 3 min into single cells and rinsed with PBS twice. Cells (1×10^7) were electroporated with appropriate combination of Cas9 plasmids (5 μg) (Addgene #44719), two gRNAs (5 μg), and CAG promoter-driven puromycin plasmid (5 μg) (Cui et al., 2016) in 200 μL of electroporation buffer using the Gene Pulser Xcell System (Bio-Rad) at 250 V and 500 μF in 0.4-cm cuvettes (Phenix Research Products). Cells were treated with puromycin (0.5 μg/mL) from day 2 to day 5 post electroporation. After puromycin selection MEF-conditioned hESCM was supplied, and drug-resistant colonies could be picked up for genotyping analyses after 10 days post electroporation. Primer sets for genomic DNA PCR are provided in Supplemental Experimental Procedures.

Immunofluorescence

Coverslip cultures were fixed in 4% paraformaldehyde at room temperature for 10 min, washed two times with PBS, and incubated for 1 hr in blocking buffer (PBS, 10% donkey serum, 0.1% Triton X-100). Cells were incubated with primary antibodies at 4°C overnight followed by three washes and stained with the fluorescently conjugated secondary antibodies (1:1,000; Jackson Laboratories) for 1 hr. Nuclei were counterstained with Hoechst 33,258 (Sigma D9542) for 5 min. Primary antibodies used in this study include the following: CTNNB1 (1:1,000; mouse immunoglobulin G [IgG], BD Biosciences 610154), and Nanog (1:2,000; goat IgG, R&D Systems AF1997).

Western Blotting

Cells were lysed in RIPA$^+$ buffer and protein concentrations were analyzed by the BCA kit (Thermo Scientific). Fifteen micrograms of total proteins was resolved on 10% SDS-PAGE gel, transferred to nitrocellulose membranes, and blotted for SMAD2/3 (1:1,000; rabbit IgG, Cell Signaling Technology #8685), CTNNB1 (1:1,000; mouse IgG, BD Biosciences 610154), GAPDH (1:2,000; rabbit IgG, Santa Cruz Biotechnology SC25778), TP53 (1:1,000; rabbit IgG, Santa Cruz SC6243). The secondary antibodies were purchased from Jackson ImmunoResearch.

Statistical Analyses

Data were analyzed using Student's t test for comparison of independent means with pooled estimates of common variances.

SUPPLEMENTAL INFORMATION

Supplemental Information includes Supplemental Experimental Procedures, four figures, and one table and can be found with this article online at http://dx.doi.org/10.1016/j.stemcr.2016.07.021.

AUTHOR CONTRIBUTIONS

Z.X., L.L., J.G., and X. L. conceived the study. L.Z., H.Y., and S.L. performed most of the experiments. C.Z., X.X., C.L., F.B., F.Y., L.Y., M.L., W.Y., and Z.Q. helped to set up the CRISPR/Cas9-mediated gene-targeting system in hPSCs. Z.Q. helped with the data analyses and proofreading of the manuscript. L.Z., H.Y., S.L., L.L., and X.Z. wrote the manuscript.

ACKNOWLEDGMENTS

This study was supported by the National Basic Research Program of China (973 Program) (2012CB966300 and 2013CB967600), the National Natural Science Foundation of China (31271588, 31471040, 31301157, 31400934, 91519323), the Ministry of Education (IRT1168), the Science and Technology Commission of Shanghai Municipality (15JC1400202, 15XD1503800), the Shanghai Municipal Education Commission (C120114), and Fundamental Research Funds for the Central Universities.

Received: February 23, 2016
Revised: July 28, 2016
Accepted: July 28, 2016
Published: September 1, 2016

REFERENCES

Brogna, S., and Wen, J.K. (2009). Nonsense-mediated mRNA decay (NMD) mechanisms. Nat. Struct. Mol. Biol. *16*, 107–113.

Byrne, S.M., Ortiz, L., Mali, P., Aach, J., and Church, G.M. (2015). Multi-kilobase homozygous targeted gene replacement in human induced pluripotent stem cells. Nucleic Acids Res. *43*, e21.

Canver, M.C., Bauer, D.E., Dass, A., Yien, Y.Y., Chung, J., Masuda, T., Maeda, T., Paw, B.H., and Orkin, S.H. (2014). Characterization of genomic deletion efficiency mediated by clustered regularly interspaced palindromic repeats (CRISPR)/Cas9 nuclease system in mammalian cells. J. Biol. Chem. *289*, 21312–21324.

Capecchi, M.R. (2005). Gene targeting in mice: functional analysis of the mammalian genome for the twenty-first century. Nat. Rev. Genet. *6*, 507–512.

Chen, H., Choi, J., and Bailey, S. (2014a). Cut site selection by the two nuclease domains of the Cas9 RNA-guided endonuclease. J. Biol. Chem. *289*, 13284–13294.

Chen, W., Liu, J., Zhang, L., Xu, H., Guo, X., Deng, S., Liu, L., Yu, D., Chen, Y., and Li, Z. (2014b). Generation of the SCN1A epilepsy mutation in hiPS cells using the TALEN technique. Sci. Rep. *4*, 5404.

Chen, X., Xu, F., Zhu, C., Ji, J., Zhou, X., Feng, X., and Guang, S. (2014c). Dual sgRNA-directed gene knockout using CRISPR/Cas9 technology in *Caenorhabditis elegans*. Sci. Rep. *4*, 7581.

Chen, Y., Cao, J., Xiong, M., Petersen, A.J., Dong, Y., Tao, Y., Huang, C.T., Du, Z., and Zhang, S.C. (2015). Engineering human stem cell lines with inducible gene knockout using CRISPR/Cas9. Cell Stem Cell *17*, 233–244.

Chi, L.K., Fan, B.B., Feng, D.D., Chen, Z.Y., Liu, Z.L., Hui, Y., Xu, X.J., Ma, L., Fang, Y.J., Zhang, Q.B., et al. (2016). The dorsoventral patterning of human forebrain follows an activation/transformation model. Cereb. Cortex. http://dx.doi.org/10.1093/cercor/bhw152.

Cho, S.W., Kim, S., Kim, J.M., and Kim, J.S. (2013). Targeted genome engineering in human cells with the Cas9 RNA-guided endonuclease. Nat. Biotechnol. *31*, 230–232.

Cong, L., Ran, F.A., Cox, D., Lin, S.L., Barretto, R., Habib, N., Hsu, P.D., Wu, X.B., Jiang, W.Y., Marraffini, L.A., et al. (2013). Multiplex genome engineering using CRISPR/Cas systems. Science *339*, 819–823.

Cui, D., Wang, J., Zeng, Y., Rao, L., Chen, H., Li, W., Li, Y., Li, H., Cui, C., and Xiao, L. (2016). Generating hESCs with reduced immunogenicity by disrupting TAP1 or TAPBP. Biosci. Biotechnol. Biochem. *80*, 1–8.

Ding, Q., Lee, Y.K., Schaefer, E.A., Peters, D.T., Veres, A., Kim, K., Kuperwasser, N., Motola, D.L., Meissner, T.B., Hendriks, W.T., et al. (2013a). A TALEN genome-editing system for generating human stem cell-based disease models. Cell Stem Cell *12*, 238–251.

Ding, Q., Regan, S.N., Xia, Y., Oostrom, L.A., Cowan, C.A., and Musunuru, K. (2013b). Enhanced efficiency of human pluripotent stem cell genome editing through replacing TALENs with CRISPRs. Cell Stem Cell *12*, 393–394.

Fatscher, T., Boehm, V., and Gehring, N.H. (2015). Mechanism, factors, and physiological role of nonsense-mediated mRNA decay. Cell Mol. Life Sci. *72*, 4523–4544.

Fu, Y., Sander, J.D., Reyon, D., Cascio, V.M., and Joung, J.K. (2014). Improving CRISPR-Cas nuclease specificity using truncated guide RNAs. Nat. Biotechnol. *32*, 279–284.

Geisinger, J.M., Turan, S., Hernandez, S., Spector, L.P., and Calos, M.P. (2016). In vivo blunt-end cloning through CRISPR/Cas9-facilitated non-homologous end-joining. Nucleic Acids Res. *44*, e76.

Genga, R.M., Kearns, N.A., and Maehr, R. (2015). Controlling transcription in human pluripotent stem cells using CRISPR-effectors. Methods *101*, 36–42.

Giudice, A., and Trounson, A. (2008). Genetic modification of human embryonic stem cells for derivation of target cells. Cell Stem Cell *2*, 422–433.

Gonzalez, F., Zhu, Z., Shi, Z.D., Lelli, K., Verma, N., Li, Q.V., and Huangfu, D. (2014). An iCRISPR platform for rapid, multiplexable, and inducible genome editing in human pluripotent stem cells. Cell Stem Cell *15*, 215–226.

Gutschner, T., Hammerle, M., and Diederichs, S. (2013). MALAT1—a paradigm for long noncoding RNA function in cancer. J. Mol. Med. *91*, 791–801.

Hendriks, W.T., Warren, C.R., and Cowan, C.A. (2016). Genome editing in human pluripotent stem cells: approaches, pitfalls, and solutions. Cell Stem Cell *18*, 53–65.

Heyer, W.D., Ehmsen, K.T., and Liu, J. (2010). Regulation of homologous recombination in eukaryotes. Annu. Rev. Genet. *44*, 113–139.

Ho, T.T., Zhou, N., Huang, J., Koirala, P., Xu, M., Fung, R., Wu, F., and Mo, Y.Y. (2015). Targeting non-coding RNAs with the CRISPR/Cas9 system in human cell lines. Nucleic Acids Res. *43*, e17.

Hockemeyer, D., and Jaenisch, R. (2010). Gene targeting in human pluripotent cells. Cold Spring Harb. Symp. Quant. Biol. *75*, 201–209.

Hockemeyer, D., Wang, H.Y., Kiani, S., Lai, C.S., Gao, Q., Cassady, J.P., Cost, G.J., Zhang, L., Santiago, Y., Miller, J.C., et al. (2011). Genetic engineering of human pluripotent cells using TALE nucleases. Nat. Biotechnol. *29*, 731–734.

Hou, Z., Zhang, Y., Propson, N.E., Howden, S.E., Chu, L.F., Sontheimer, E.J., and Thomson, J.A. (2013). Efficient genome engineering in human pluripotent stem cells using Cas9 from *Neisseria meningitidis*. Proc. Natl. Acad. Sci. USA *110*, 15644–15649.

Hsu, P.D., Scott, D.A., Weinstein, J.A., Ran, F.A., Konermann, S., Agarwala, V., Li, Y., Fine, E.J., Wu, X., Shalem, O., et al. (2013). DNA targeting specificity of RNA-guided Cas9 nucleases. Nat. Biotechnol. *31*, 827–832.

Hsu, P.D., Lander, E.S., and Zhang, F. (2014). Development and applications of CRISPR-Cas9 for genome engineering. Cell *157*, 1262–1278.

Hu, B.Y., Weick, J.P., Yu, J., Ma, L.X., Zhang, X.Q., Thomson, J.A., and Zhang, S.C. (2010). Neural differentiation of human induced pluripotent stem cells follows developmental principles but with variable potency. Proc. Natl. Acad. Sci. USA *107*, 4335–4340.

Ivey, K.N., and Srivastava, D. (2010). MicroRNAs as regulators of differentiation and cell fate decisions. Cell Stem Cell *7*, 36–41.

Jasin, M., and Rothstein, R. (2013). Repair of strand breaks by homologous recombination. Cold Spring Harbor Perspect. Biol. *5*, a012740.

Jia, W., Chen, W., and Kang, J. (2013). The functions of microRNAs and long non-coding RNAs in embryonic and induced pluripotent stem cells. Genomics Proteomics Bioinformatics *11*, 275–283.

Jinek, M., Chylinski, K., Fonfara, I., Hauer, M., Doudna, J.A., and Charpentier, E. (2012). A programmable dual-RNA-guided DNA endonuclease in adaptive bacterial immunity. Science *337*, 816–821.

Kang, H., Minder, P., Park, M.A., Mesquitta, W.T., Torbett, B.E., and Slukvin, I.I. (2015). CCR5 disruption in induced pluripotent stem cells using CRISPR/Cas9 provides selective resistance of immune cells to CCR5-tropic HIV-1 virus. Mol. Ther. Nucleic Acids *4*, e268.

Kleinstiver, B.P., Pattanayak, V., Prew, M.S., Tsai, S.Q., Nguyen, N.T., Zheng, Z.L., and Joung, J.K. (2016). High-fidelity CRISPR-Cas9 nucleases with no detectable genome-wide off-target effects. Nature *529*, 490–495.

Lackner, D.H., Carre, A., Guzzardo, P.M., Banning, C., Mangena, R., Henley, T., Oberndorfer, S., Gapp, B.V., Nijman, S.M., Brummelkamp, T.R., et al. (2015). A generic strategy for CRISPR-Cas9-mediated gene tagging. Nat. Commun. *6*, 10237.

Lee, H.J., Kim, E., and Kim, J.S. (2010). Targeted chromosomal deletions in human cells using zinc finger nucleases. Genome Res. *20*, 81–89.

Lv, Q., Lai, L., Yuan, L., Song, Y., Sui, T., and Li, Z. (2016). Tandem repeat knockout utilizing the CRISPR/Cas9 system in human cells. Gene *582*, 122–127.

Lykke-Anderson, S., and Jensen, T.H. (2015). Nonsense-mediated mRNA decay: an intricate machinery that shapes transcriptomes. Nat. Rev. Mol. Cell Biol. *16*, 665–677.

Mali, P., and Cheng, L. (2012). Concise review: human cell engineering: cellular reprogramming and genome editing. Stem Cells *30*, 75–81.

Mali, P., Esvelt, K.M., and Church, G.M. (2013). Cas9 as a versatile tool for engineering biology. Nat. Methods *10*, 957–963.

Mandal, P.K., Ferreira, L.M., Collins, R., Meissner, T.B., Boutwell, C.L., Friesen, M., Vrbanac, V., Garrison, B.S., Stortchevoi, A., Bryder, D., et al. (2014). Efficient ablation of genes in human hematopoietic stem and effector cells using CRISPR/Cas9. Cell Stem Cell *15*, 643–652.

Pauli, A., Rinn, J.L., and Schier, A.F. (2011). Non-coding RNAs as regulators of embryogenesis. Nat. Rev. Genet. *12*, 136–149.

Shalem, O., Sanjana, N.E., Hartenian, E., Shi, X., Scott, D.A., Mikkelsen, T.S., Heckl, D., Ebert, B.L., Root, D.E., Doench, J.G., et al. (2014). Genome-scale CRISPR-Cas9 knockout screening in human cells. Science *343*, 84–87.

Slaymaker, I.M., Gao, L., Zetsche, B., Scott, D.A., Yan, W.X., and Zhang, F. (2016). Rationally engineered Cas9 nucleases with improved specificity. Science *351*, 84–88.

Song, Y., Yuan, L., Wang, Y., Chen, M., Deng, J., Lv, Q., Sui, T., Li, Z., and Lai, L. (2016). Efficient dual sgRNA-directed large gene deletion in rabbit with CRISPR/Cas9 system. Cell Mol. Life Sci. *73*, 2959–2968.

Stemmer, M., Thumberger, T., Del Sol Keyer, M., Wittbrodt, J., and Mateo, J.L. (2015). CCTop: an intuitive, flexible and reliable CRISPR/Cas9 target prediction tool. PLoS One *10*, e0124633.

Wang, T., Wei, J.J., Sabatini, D.M., and Lander, E.S. (2014). Genetic screens in human cells using the CRISPR-Cas9 system. Science *343*, 80–84.

Xiao, A., Wang, Z., Hu, Y., Wu, Y., Luo, Z., Yang, Z., Zu, Y., Li, W., Huang, P., Tong, X., et al. (2013). Chromosomal deletions and inversions mediated by TALENs and CRISPR/Cas in zebrafish. Nucleic Acids Res. *41*, e141.

Zhang, S.C., Wernig, M., Duncan, I.D., Brustle, O., and Thomson, J.A. (2001). In vitro differentiation of transplantable neural precursors from human embryonic stem cells. Nat. Biotechnol. *19*, 1129–1133.

Zhang, X., Huang, C.T., Chen, J., Pankratz, M.T., Xi, J., Li, J., Yang, Y., Lavaute, T.M., Li, X.J., Ayala, M., et al. (2010). Pax6 is a human neuroectoderm cell fate determinant. Cell Stem Cell *7*, 90–100.

Zhang, L., Jia, R., Palange, N.J., Satheka, A.C., Togo, J., An, Y., Humphrey, M., Ban, L., Ji, Y., Jin, H., et al. (2015). Large genomic fragment deletions and insertions in mouse using CRISPR/Cas9. PLoS One *10*, e0120396.

Zheng, Q., Cai, X., Tan, M.H., Schaffert, S., Arnold, C.P., Gong, X., Chen, C.Z., and Huang, S. (2014). Precise gene deletion and replacement using the CRISPR/Cas9 system in human cells. Biotechniques *57*, 115–124.

Zhou, J., Wang, J., Shen, B., Chen, L., Su, Y., Yang, J., Zhang, W., Tian, X., and Huang, X. (2014). Dual sgRNAs facilitate CRISPR/Cas9-mediated mouse genome targeting. FEBS J. *281*, 1717–1725.

Zwaka, T.P., and Thomson, J.A. (2003). Homologous recombination in human embryonic stem cells. Nat. Biotechnol. *21*, 319–321.